http://ansinet.com/itj

ITJ

ISSN 1812-5638

INFORMATION TECHNOLOGY JOURNAL

ANSInet
Asian Network for Scientific Information
308 Lasani Town, Sargodha Road, Faisalabad - Pakistan

Information Technology Journal 12 (23): 7319-7324, 2013
ISSN 1812-5638 / DOI: 10.3923/itj.2013.7319.7324

Analysis and Study of the Obstacle Crossing Ability of Wheel-crawler Compound Mobile Robot

Jianjun Qin, Rui Ma, Yan Hua, Jianwei Yang
School of Mechanical-electronic and Vehicle Engineering,
Beijing University of Civil Engineering and Architecture, 100044 Beijing, China

Abstract: The obstacle crossing ability under complicated terrain environment is the key and difficult point during design of small mobile robots and the common approach is to realize this ability through combination of multiple marching forward methods. This study conducts detailed analysis of the obstacle crossing performance of a new wheels-crawler compound robot. The robot includes multiple movement forms such as common wheel movement, crawler running and crawler swinging movement and through obstacle crossing ability analysis of various movement forms under typical terrain environment, it could provide theoretic support to the design of robot. The research results show that this robot has both the ability of fast movement on smooth road and obstacle crossing ability under non-structural terrain environment.

Key words: Terrain environment, obstacle crossing ability, wheel type, crawler type, complicated terrain

INTRODUCTION

The marching forward device of mobile robot mainly includes the wheel type, crawler type, leg type and their compound form (Adachi *et al*., 1999). Through research, we find that current small mobile robots generally have the problem of low adaptability to complicated terrain environment, i.e., if it has high obstacle crossing performance, it has low motility; or if it satisfies the requirement of high flexibility, it lacks high obstacle crossing ability (Michaud *et al*., 2005). Therefore, it is very necessary to design a small portable robot with both high obstacle crossing ability and high motility (Saranli *et al*., 2001; Guccione and Muscato, 2003; Chou and Yang, 2013).

Based on the proposal of a new wheel-crawler compound mobile robot, this study conducts analysis of its obstacle crossing performance and this robot mainly has two working modes of wheel mode and crawler mode. It also has three working states when driven by the crawler, which are pure rolling of crawler, pure swinging of arm and the overall combination of rolling and swinging. Under the pure rolling state of crawler, the robot can adapt to complicated terrain. Under the pure swinging state, the robot can have multiple postures, which can change the robot's center of gravity to further improve the robot's obstacle crossing ability. The combination of rolling and swinging is definitely the highest state of obstacle crossing performance, which can adapt to more severe terrain environment.

CONCEPT DESIGN OF ROBOT

The proposed design scheme for new robot is as shown in Fig. 1. The robot adopts compound drive, one mode is wheel drive and the other is crawler drive. When it is required to switch mode, a deformation device is used to shove off the outer circle of wheel and turn it into the crawler. Under the crawler drive mode, the swimming of crawler can be controlled through the swing arm, in this way to increase its obstacle crossing ability.

Under normal operation, the robot is under the wheel mode, as shown in Fig. 1a. When it is required to pass a complicated terrain, the wheels will change into four independent mechanical arms, as shown in Fig. 1b. When the mechanical arms have rotation, only the crawler on the mechanical arm will rotate, just like the way a common crawler robot passes a complicated terrain. When the mechanical arms have rotation plus revolution, the robot conducts compound movement of crawler rotation and swing arm movement and it can pass high steps through the rotation of swing arms. Because the four mechanical arms can swing independently, it can pass extremely complicated terrain, such as soft and thick snow. In the meantime, when the robot rolls over or gets stuck, it can lift itself up through the swing arm, which can significantly improve the robot's movement ability on the road.

Corresponding Author: Jianjun Qin, School of Mechanical-electronic and Vehicle Engineering,
Beijing University of Civil Engineering and Architecture, 100044 Beijing, China, Tel: 86-10-68322420

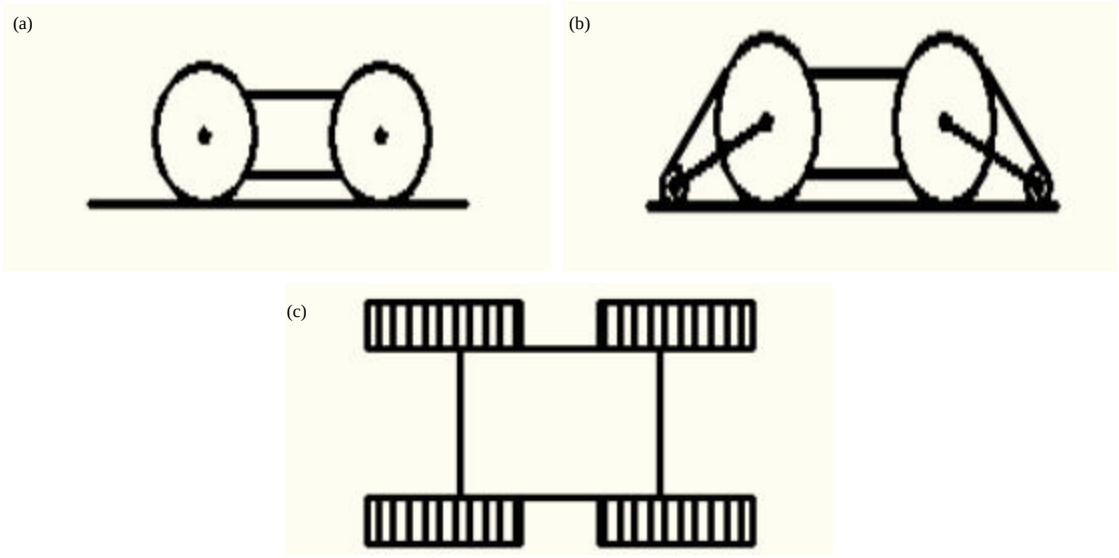

Fig. 1(a-c): Sketch of the wheel-crawler compound robot

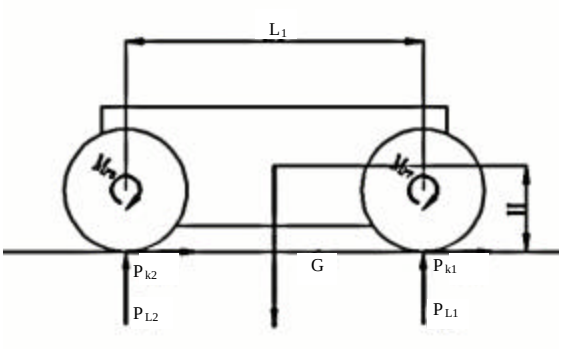

Fig. 2: Force analysis diagram of planar motion

WHEEL-TYPE STRAIGHT MOVEMENT

The force analysis schematic diagram of a mobile robot moving on a flat surface is as shown in Fig. 2 and the total moving resistance is:

$$F_1 = F_f + F_\alpha$$

$$F_f = \mu G$$

$$F_\alpha = ma$$

where, F_f-rolling resistance; F_α-acceleration resistance; μ-coefficient of rolling friction; α-required acceleration on flat surface.

When the robot moves with the maximum speed v_{max} on the flat surface, the required power P_1 to drive the robot is:

$$P_1 = \frac{F_f v_{max}}{1000\eta_L}$$

where, v_{max}-maximum moving speed on the flat surface, take $v_{max} \geq 7$ m sec^{-1}; η-drive efficiency of working machine (wheel/crawler).

Make $\eta_L = 1$ and $\eta_U = 0.94\sim0.96$ (with transmission).

We can get the required power of motor P_1 is:

$$P_{1'} = P_1/4$$

When the robot moves with the maximum speed v_{max} on the flat surface, the mechanical axis O_1 has an angular velocity n_{Lz} as:

$$n_{Lz} = \frac{30\, v_{max}}{pR}$$

where, R-radius of the wheel.

When the robot moves with the maximum speed v_{max} on the flat surface, the mechanical axis O_1 is under the torque T_{Lz} of:

$$T_{Lz} = \frac{F_f R}{4}$$

When the robot starts on the flat surface, the mechanical axis O_1 has a maximum starting load demand torque T_{Lmax} of:

$$T_{Lzmax} = \frac{(F_f + F_a)R}{4}$$

And:

$$T_{Lzmax} = \frac{(\mu G + ma)R}{4}$$

On the flat surface, the mechanical axis O_1 has a minimum starting load demand torque T_{smin} of:

$$T_{LzSmin} = \frac{T_{Lzmax} K_s}{K_u}$$

Where, K_s--the coefficient that ensures that there is adequate accelerating torque during starting, which is generally between 1.15~1.25; K_u--voltage fluctuation coefficient, i.e., the ratio between the motor side voltage and rated voltage, which is 0.85 during full-voltage starting.

WHEEL-TYPE CLIMBING MOVEMENT

The typical posture of robot during climbing is as shown in Fig. 3 and when the robots moves with a uniform velocity in an angle of α, the total moving resistance on the ramp f_2 is:

$$f_2 = F_f + F_i = G(\sin a + \mu \cos a)$$

where, F_f-rolling resistance; F_i-grade resistance.

When the robot moves with a uniform velocity on a ramp with an angle of α, the mechanical axis O_1 is under the torque T_{Lp} of:

$$T_{Lp} = \frac{f_2 R}{4}$$

When the robot moves with a uniform velocity on a ramp with an angle of α, the mechanical axis O_1 and wheel speed n_{Lp} are:

$$n_{Lp} = \frac{30\, v_i}{pR}$$

where, R--radius of wheel; v_i-the speed to climb up steps and average slope, which is generally $v_i \geq 1.2$ m sec^{-1}.

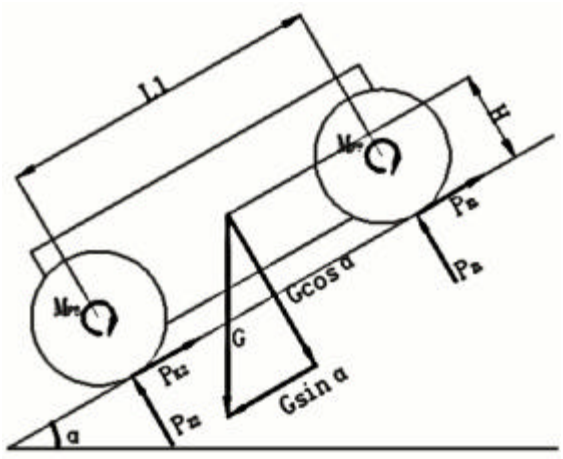

Fig. 3: Climbing posture of robot

When the robot moves with a uniform velocity on a ramp with an angle of α, the required power p_2 by the robot is:

$$P_2 = \frac{f_2 V_i}{1000 \eta_L}$$

When the robot moves with a uniform velocity on a ramp with an angle of α, the required power P_2 by the mechanical axis O_1 is:

$$P_2' = \frac{T_{Lp} n_{Lp}}{9550 \eta_L}$$

In accordance with the chassis size and specification, we obtain the maximum theoretical climbing angle α_{Lmax} is:

$$a_{Lmax} = \arcsin \frac{h}{\sqrt{l^2 + h^2}}$$

When the robot moves with a uniform velocity on a ramp with an angle of α_{Lmax}, the mechanical axis O_1 has a maximum climbing load torque T_{Lpmax} of:

$$T_{Lpmax} = \frac{G(\sin a_{Lpmax} + \mu \cos a_{Lpmax})R}{4}$$

CRAWLER-TYPE FLAT MOVEMENT

The movement of robot in crawler mode on flat surface is as shown in Fig. 4 and the moving resistance f_4 in crawler mode is:

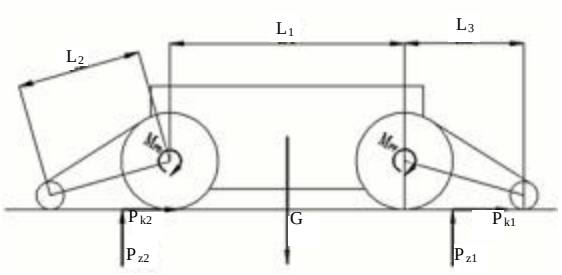

Fig. 4: Flat movement of robot in crawler mode

$$f_4 = F_a + F_i + F_c + f_\eta$$

where, F_a-acceleration resistance; F_i-gradient resistance; F_c-soil compaction resistance; f_η-internal mechanic resistance.

Where, internal mechanic resistance f_η is reflected in the formula as mechanical efficiency.

The soil compaction resistance F_c is actually caused by the consumed energy by compacting soil and forming tracks, so it can be calculated through function transformation. When the crawler-type robot moves forward a distance of L_3 (L_3 is the length of crawler contacting the ground), the power P consumed by robot for compacting soil is:

$$P = \int_0^{z_0} 2bL_3 p dz$$

where, b-crawler width; P-load on unit bearing area of soil; Z_0-track depth.

When the robot moves forward a distance of L, the consumed power $F_C \bullet L_3$ to overcome the soil compaction resistance F_C should equal to the power P of robot compacting soil, so:

$$F_C L_3 = P = 2bL_3 \int_0^{z_0} p dz$$

$$F_C = 2b \int_0^{z_0} p dz$$

In accordance with the pressure settlement Eq:

$$p = kz^n$$

where, K-soil deformation modulus; n-soil deformation index. (Liu and Pei, 2005; 2006).

So:

$$F_C = 2b \int_0^{z_0} kz^n dz = 2bk \frac{Z_0^{n+1}}{n+1}$$

where, F_c can be further related to the machine parameters through Z_0. Assume the ground contact pressure of crawler is evenly distributed, when the soil is deeply compacted by Z_0, the unit area of soil bears a pressure of p_{cp} (average ground contact pressure):

$$p_{cp} = \frac{G}{2bL_3} = \frac{G}{A}$$

where, G-machine weight; n-ground contact area of crawler.

So:

$$Z_0 = \left(\frac{p_{cp}}{K}\right)^{\frac{1}{n}} = \left(\frac{G}{KA}\right)^{\frac{1}{n}}$$

$$F_C = \frac{2b}{(n+1)K^{\frac{1}{n}}}\left(\frac{G}{A}\right)^{\frac{n+1}{n}} = \frac{2b}{(n+1)K^{\frac{1}{n}}}\left(p_{cp}\right)^{\frac{n+1}{n}}$$

When we calculate the soil compaction resistance F_c, we use Rayleigh-Jeans Eq:

$$p = \left(CK_c' + \frac{?b}{2}K_f'\right)\left(\frac{z}{b}\right)^n$$

Then, we have:

$$F_C = \frac{2b^2}{(n+1)^n \sqrt{CK_c' + \frac{?b}{2}K_f'}}\left(\frac{G}{A}\right)^{\frac{n+1}{n}}$$

Assume the ground contact pressure of crawler is not evenly distributed and set the horizontal eccentric distance as c and longitudinal eccentric distance as e:

$$F_C = \frac{b}{(n+1)K^{\frac{1}{n}}}\left[p_{cp}\left(1+\frac{6e}{L}\right)\right]^{\frac{n+1}{n}}$$

$$\left[\left(1+\frac{2c}{B}\right)^{\frac{n+1}{n}} + \left(1-\frac{2c}{B}\right)^{\frac{n+1}{n}}\right]$$

CRAWLER-TYPE CLIMBING MOVEMENT

When the robots moves with a uniform velocity in an angle of α, the total moving resistance on the ramp f_4 is:

$$f_4 = F_i + F_c + f_?$$

where, F_i-grade resistance; f_c-soil compaction resistance; f_η-internal mechanic resistance (Fig. 5).

In the meantime, we can know:

$$f_4 = \frac{2b^2}{(n+1)^n\sqrt{CK_c' + \frac{?b}{2}K_f'}}\left(\frac{Gcosa}{A}\right)^{\frac{n+1}{n}} + Gsina$$

When the robot moves with a uniform velocity of v_i required by climbing on a ramp with an angle of α, the mechanical axis O_1 is under the torque of:

$$T_{Up} = \frac{f_4 R}{4}$$

When the robot moves with a uniform velocity of v_i required by climbing on a ramp with an angle of α, the mechanical axis O_1 and the wheel speed n_{Up} are:

$$n_{Up} = \frac{30\ v_i}{pR}$$

where, R--radius of wheel; v_i-the speed to climb up steps and average slope, which is generally $v_i \geq 1.2\ m\ sec^{-1}$.

When the robot moves with a uniform velocity of v_i required by climbing on a ramp with an angle of α, the power P_2 required by the robot is:

$$P_3 = \frac{f_4 v_i}{1000?_U?}$$

where, η--overall efficiency of transmission device.

Select the value of 0.7 during the period of dynamic calculation and select the value in accordance with the actual design scheme of transmission device after motor model selection:

$$P_3 = \frac{\left[\frac{2b^2}{(n+1)^n\sqrt{CK_c' + \frac{?b}{2}K_f'}}\left(\frac{Gcosa}{A}\right)^{\frac{n+1}{n}} + Gsina\right] v_i}{1000?_U?}$$

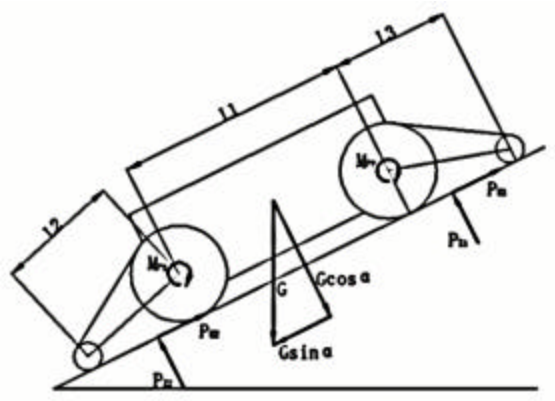

Fig. 5: Climbing movement of robot in crawler mode

When the robot moves with a uniform velocity of v_i required by climbing on a ramp with an angle of α, the power P_3 required by the mechanical axis O_1 is:

$$P_3' = \frac{T_{Up} n_{Up}}{9550?_U?}$$

Then, we have:

$$P_3' = \frac{\left[\frac{2b^2}{(n+1)^n\sqrt{CK_c' + \frac{?b}{2}K_f'}}\left(\frac{Gcosa}{A}\right)^{\frac{n+1}{n}} + Gsina\right] Rn_{LO1}}{38200?_U?}$$

Through organization, we obtain:

$$P_3' = \frac{3\left[\frac{2b^2}{(n+1)^n\sqrt{CK_c' + \frac{?b}{2}K_f'}}\left(\frac{Gcosa}{A}\right)^{\frac{n+1}{n}} + Gsina\right] v_i}{7640p^2?_U?}$$

In accordance with the chassis size and specification, we obtain the maximum theoretical climbing angle α_{Upmax} of crawler; when the robot moves with a uniform velocity on a ramp with an angle of α_{Upmax}, the mechanical axis O_1 has a maximum climbing load torque T_{Upmax} of:

$$T_{Upmax} = \frac{\left[\frac{2b^2}{(n+1)^n\sqrt{CK_c' + \frac{?b}{2}K_f'}}\left(\frac{Gcosa_{Dmax}}{A}\right)^{\frac{n+1}{n}} + Gsina_{Dmax}\right] R}{4}$$

CONCLUSION

Through analysis of the obstacle-crossing process of robot, we find it can adapt to most categories of terrain environment. Because it has high mobility and obstacle-crossing ability, this robot can be applied in multiple fields, which has huge development potential.

ACKNOWLEDGMENTS

This study is supported by the supported by Beijing University Youth Talent Program (Project number: YETP1656), Great Wall Scholars Training Program in Institutions of Higher Learning Under the Jurisdiction of Beijing Municipality (Project number: CIT and TCD20140311), Funding Project for Academic Human Resources Development in Institutions of Higher Learning Under the Jurisdiction of Beijing Municipality (Project number: 201106125) and by Open Research Fund Program of Beijing Engineering Research Center of Monitoring for Construction Safety (Beijing University of Civil Engineering and Architecture).

REFERENCES

Adachi, H., N. Koyachi, T. Arai, A. Shimiza and Y. Nogami, 1999. Mechanism and control of a leg-wheel hybrid mobile robot. Proceedings of the IEEE/RSJ International Conference on Intelligent Robots and Systems, October 7-21, 1999, Kyongju, pp: 1792-1797.

Chou, J.J. and L.S. Yang, 2013. Innovative design of a claw-wheel transformable robot. Proceedings of the International Conference on Robotics and Automation, May 6-10, 2013, Karlsruhe, pp: 1337-1342.

Guccione, S. and G. Muscato, 2003. The wheeleg robot. IEEE Robot. Automat. Mag., 10: 33-43.

Liu, Y. and P. Pei, 2005. Analysis on ignition and extinction of n-heptane in homogeneous systems. Sci. China Series E Eng. Mater. Sci., 48: 556-569.

Liu, Y. and P. Pei, 2006. Asymptotic analysis on autoignition and explosion limits of hydrogen-oxygen mixtures in homogeneous systems. Int. J. Hyd. Energy, 31: 639-647.

Michaud, F., D. Letourneau, M. Arsenault, Y. Bergeron and R. Cadrin et al., 2005. Multi-modal locomotion robotic platform using leg-track-wheel articulations. Autonomous Robots, 18: 137-156.

Saranli, U., M. Buehler and D.E. Koditschek, 2001. Rhex: A simple and highly mobile hexapod robot. Int. J. Robot. Res., 20: 616-631.